JOURNAL OF MATERIALS SCIENCE 20 (1985) 4027–4034

Visualization of antiferromagnetic domain structures on as-grown NiO crystals by optical methods

HIROSHI KOMATSU*, MAREO ISHIGAME‡
*The Research Institute for Iron, Steel and Other Metals and ‡The Research Institute for Scientific Measurements, Tohoku University, Sendai 980, Japan

The antiferromagnetic T-domain structures on a bulk NiO crystal surface could be visualized by means of incident-light types of microscope such as a differential interference microscope, a phase-contrast microscope and a high-dispersion interference contrast method. The visualization of the antiferromagnetic domain is possible due to the facial tilt which was induced in the NiO crystal due to the antiferromagnetic ordering below the Néel temperature. The lateral resolution of the present methods in visualization of the domain structure is about 1 μm, which is better than that of X-ray or neutron topography. The tilt angle between each domain was measured by two-beam interferometry; the average experimental value (9′23″) agrees fairly well with the calculated value (8′24″). Direct observation of the movement and disappearance of the domain boundaries upon heating could also be carried out under the phase-contrast microscope.

1. Introduction

Nickel oxide (NiO) is an antiferromagnetic material below the Néel temperature (T_N) of 523 K [1, 2], and paramagnetic above this temperature with the NaCl structure [3, 4]. At temperatures below T_N an antiferromagnetic ordering takes place and the crystal structure is slightly contracted along one of the $\langle 1\,1\,1 \rangle$ axes; thus the structure becomes rhombohedral, and if a unit cell containing four NiO molecules is used the rhombohedral angle α becomes 90°4.2′ at 297 K [5]. The rhombohedral distortion is so small that the crystallographic orientation for the twinning structure can be conventionally described referring to the parent cubic lattice as used by Roth [6]. This distortion brings about strain, which is relaxed by forming a twinning structure whose twinning planes have been worked out to be either $\{1\,0\,0\}$ or $\{1\,1\,0\}$ with respect to the parent cubic lattice. The twinning boundary coincides with the antiferromagnetic domain wall, hence the name T(twin)-domain wall [5, 6].

The optical observation of the T-wall has been carried out on thin sections of NiO by polarized light transmitted through the specimen [6]. Slack [5] observed the antiferromagnetic domain boundaries on a well-annealed cleavage face by a specular reflection technique. X-ray topographic observations of the T-walls have also been made [7–10].

The present paper reports new methods for the visualization of the antiferromagnetic T-wall domain structures on the surface of bulk NiO crystals. Well-established surface microtopographic methods [11] such as the incident type phase-contrast microscope (PCM), a differential interference microscope (DIM) and a high-dispersion interference contrast method were used for the observation. The facial tilt angle between the antiferromagnetic domains has been measured by two-beam interferometry (TBI) for the first time.

2. Results

A smooth (1 0 0) surface of NiO crystal of more

0022–2461/85 $03.00 + .12

Figure 1 Antiferromagnetic twinning domains on the as-grown (1 0 0) surface, photographed by DIM. The dendrite on the left shows predominant two-wall domains and the one on the right shows four-wall domains.

than 10 mm^2 area was prepared by melting NiO powder (purity 99.9%) using a solar furnace [12]. On the as-grown surface many dendritic patterns and several small optically flat areas were seen with the naked eye, and when they were examined with incident light using DIM or PCM, various types of antiferromagnetic domain pattern were clearly revealed. In order to confirm that they were the real antiferromagnetic domains a heating experiment was conducted as will be mentioned later. Fig. 1 is an example of such domain patterns observed by DIM on the as-grown (1 0 0) surface of the dendrites, whose antiferromagnetic lamellar twins develop in several directions. The crystallographic orientation of the antiferromagnetic twinning planes on the (1 0 0) surface was determined to be either $\{0\,0\,1\}$ or $\{0\,1\,1\}$ planes with respect to the cleavage plane which is parallel to the (0 1 0) plane; furthermore, the same surface was etched and the crystallographic orientation was reconfirmed by the etch figures [13].

As shown in Fig. 2, the straight lines which run through the whole of the (1 0 0) surface both in the vertical and horizontal directions are the traces of the cleavage lines which are parallel to [0 0 1] and [0 1 0] respectively, therefore the extending orientation of the narrow twinning domains in Fig. 2 is determined to be parallel to the $[0\,\bar{1}\,\bar{1}]$ direction as a whole. Only occasionally they shift to the $[0\,1\,\bar{1}]$ direction to a small amount, but soon return to the $[0\,\bar{1}\,\bar{1}]$ direction again. Thus this surface consists mainly of the two-wall twin structure and is only partly modified by the four-wall twin structure [5, 6]. Fig. 3 is an enlarged photomicrograph of such two-wall domains taken by an incident DIM. The photomicrograph shown in Fig. 4 is a clear four-

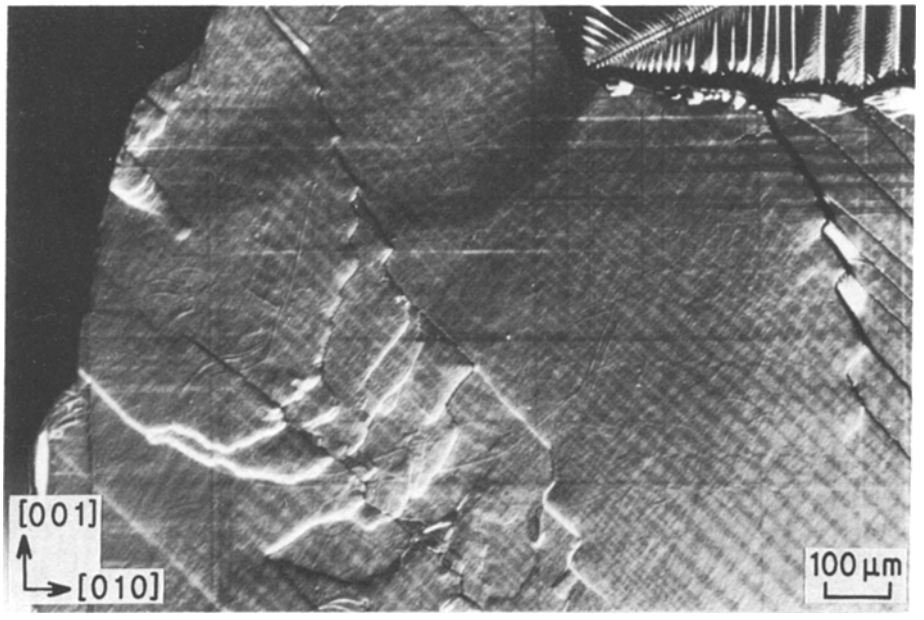

Figure 2 Antiferromagnetic lamellar twins of the two-wall twinning type and cleavage lines on the (1 0 0) surface, photographed by DIM.

wall twin pattern whose idealized orientation relationship is schematically shown in Fig. 5, in which the same nomenclature that was used by Slack [5] and Roth [6] was adopted. Many irregular fine lines in Fig. 4 are the thin growth markings left on the surface in the solidification process.

So far we have seen simple domain patterns, but in reality there were a variety of complex domain patterns derived from a combination of several twinning planes as shown in the DIM photomicrograph of Fig. 6, which is composed of the four-wall domains intersecting each other. Some of the as-grown surface shows more

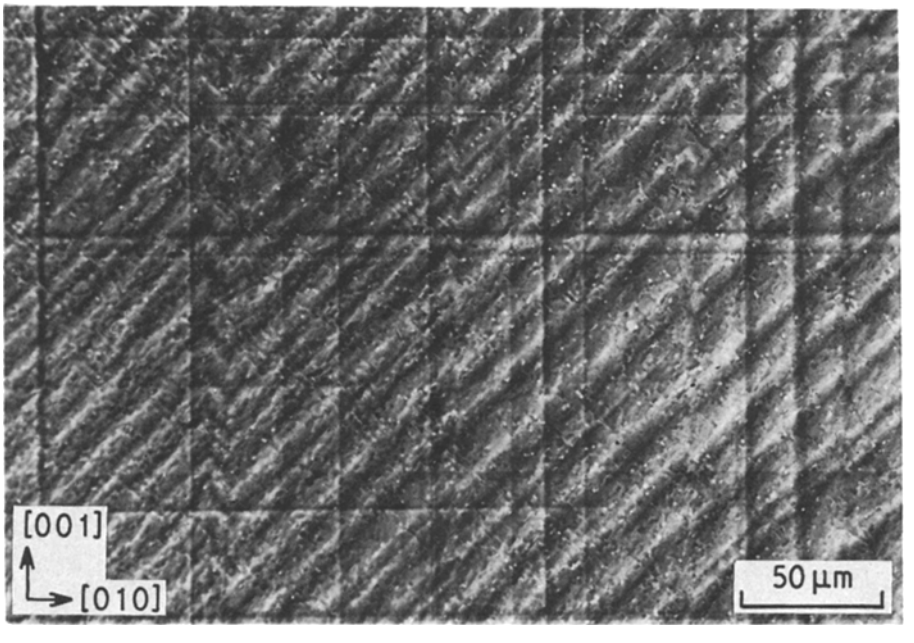

Figure 3 The two-wall twinning structure on the (1 0 0) surface with small amount of four-wall structure, photographed by PCM with a × 20 negative-contrast objective lens. The horizontal and vertical straight lines are the traces of cleavage planes.

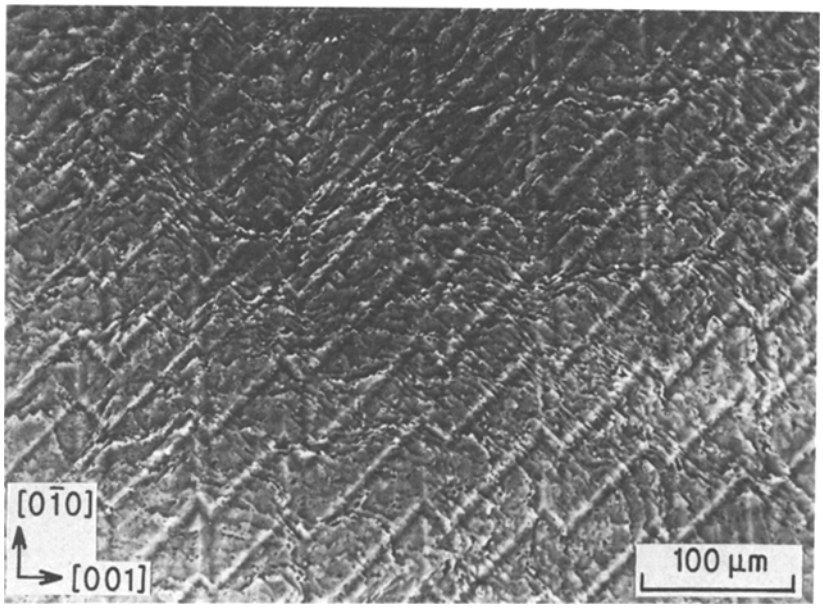

Figure 4 A typical four-wall twinning structure on the (1 0 0) surface taken by PCM with a × 20 negative-contrast objective lens.

complicated twinning structures, composed of a mixture of various domains whose orientations and dimensions are different to each other as can be seen in Fig. 7, which was taken by PCM. The origin of these complicated domain structures may be ascribed to uneven thermal stress during solidification. It should be emphasized here that a high resolution was attained in detecting a small domain whose width was less than 3 μm as shown in Fig. 7.

Direct observation of the movement of the twin boundaries during heat treatment was carried out using DIM or PCM. The specimen (Fig. 8a) was warmed up by resistance heating using a Nichrome wire wound around the sample. The facial tilt angle diminished as the temperature was increased and completely disappeared above the Néel temperature as shown in Fig. 8b. The domain pattern appeared again when the temperature was decreased below T_N, but the pattern was usually altered to a more irregular form due to the thermal stress, which may be unevenly induced either in the heating or in the cooling process. Fig. 8a shows the crystallographic orientation relation between the cleavage lines and the two-wall domain boundaries, which are faintly visible with many white lines which intersect the cleavage lines at 45° as in the case of Fig. 2 or Fig. 3. The white irregular patterns both in the right hand side and in the middle of Figs. 8a and b are the edges of the dendritic layers which were formed in the solidification process. Fig. 8b was photographed when the specimen was kept above T_N, at which no antiferromagnetic domain walls could survive, therefore only the growth markings and the cleavage lines are seen.

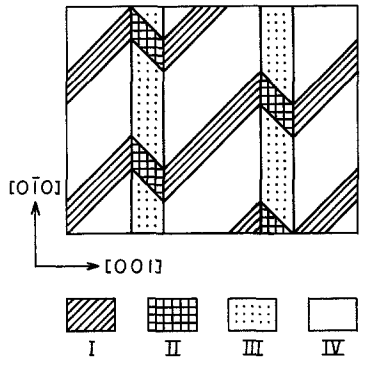

Figure 5 Schematic drawing of the four-wall twinning structure.

It was possible to visualize the antiferromagnetic domains by using highly dispersed two-beam interference fringes [14] on an as-grown surface as shown in Fig. 9. The facial tilt angle θ of the two-wall twin domains (a small amount of four-wall twin domain was intermixed) was

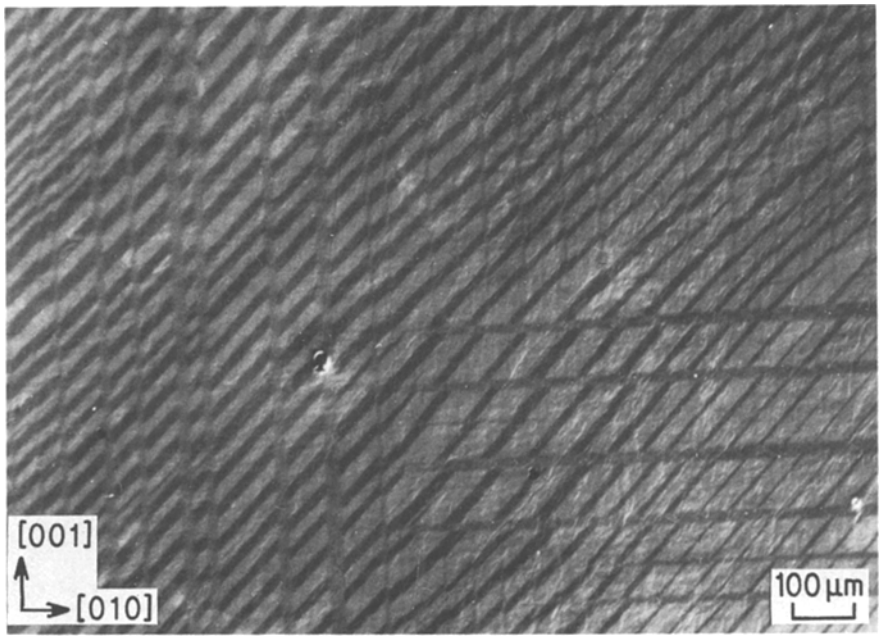

Figure 6 Intersecting four-wall twinning structures on the (1 0 0) surface taken by DIM.

estimated from the measurement of the height h and width w of the lamellar twins ($\theta = \tan^{-1} h/w$) by means of TBI (using a Nikon Surface Finish microscope), with monochromatic light of wavelength 546 nm (Fig. 10). It is clearly shown that the height and width of the domains are quite variable. The average height and width of each lamella measured from the interferogram were 30 nm and 11 μm respectively. Therefore the average facial tilt angle between the twin domain boundaries in Fig. 10 was 9′23″, which agrees fairly well with the value 8′24″ calculated from the values shown in Table I of Slack's paper [5].

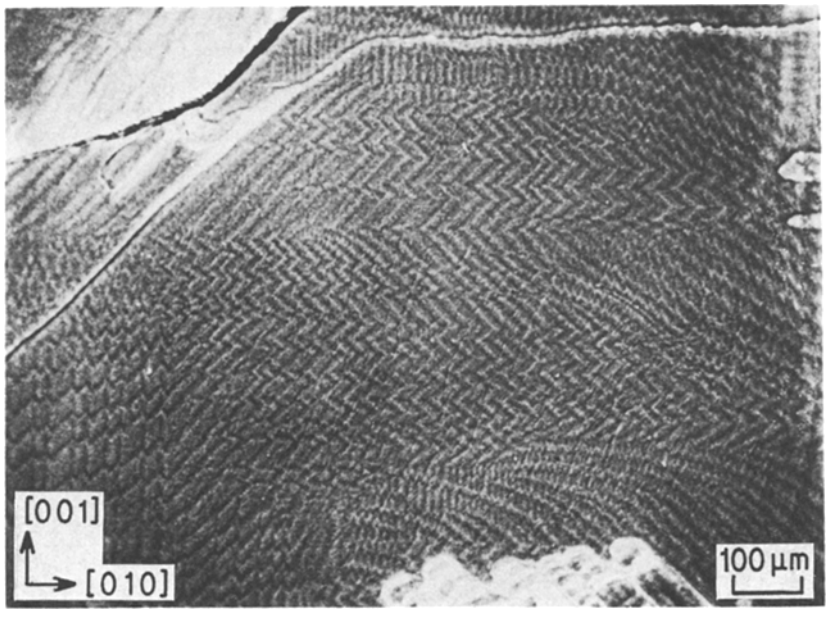

Figure 7 Intermixed four-wall domains on an as-grown (1 0 0) surface taken by a × 10 PCM negative-contrast objective lens.

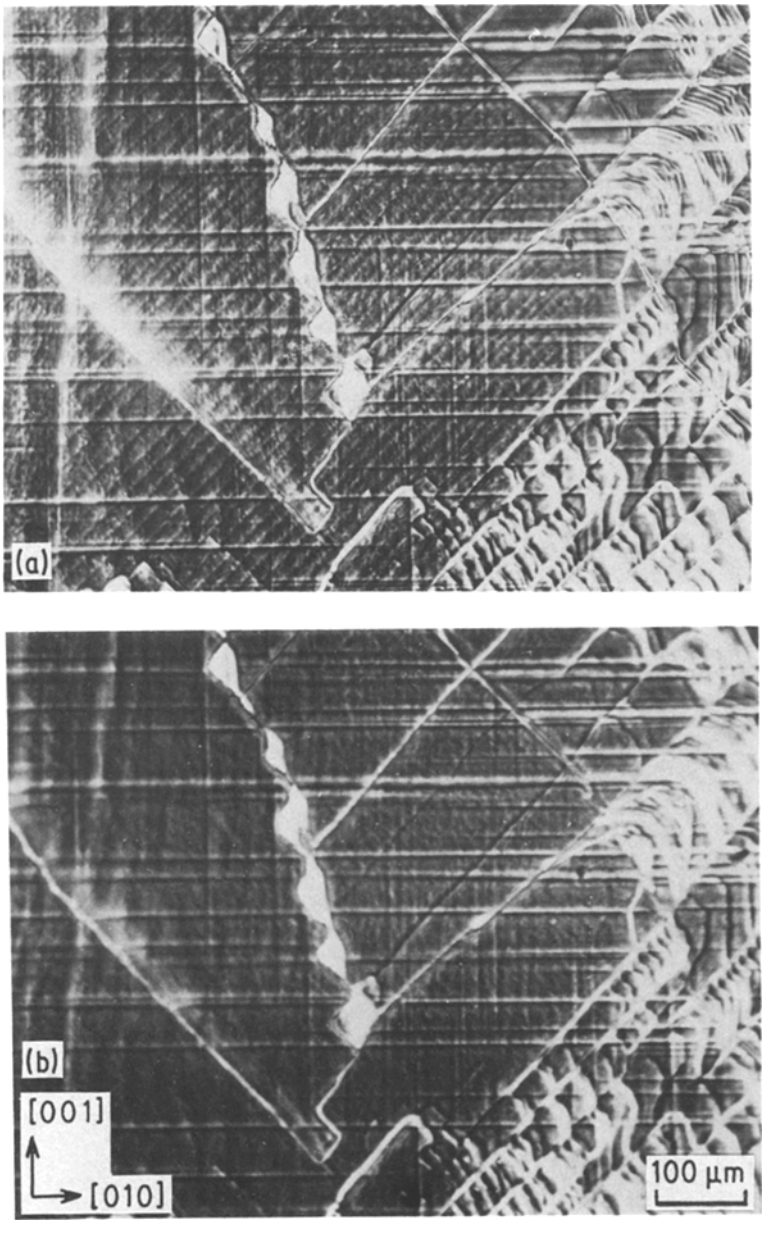

Figure 8 (a) Fine lamellar twinnings parallel to the [1 1 0] direction on the (1 0 0) surface below T_N. Straight cleavage lines and irregular growth markings are also seen. (PCM with a $\times 10$ negative-contrast objective lens). (b) No lamellar twinnings exist when heated up above T_N. (PCM with the same objective lens as Fig. 8a).

3. Discussion

Surface microtopographic methods such as DIM, PCM and TBI are suited to the observation of the antiferromagnetic domain boundaries on any surface as long as a surface distortion exists. Therefore the T-walls can be detected by the present method but the S-walls [5, 6, 15], which may not accompany detectable surface distortion, will not be seen by these methods.

The detection limit of the facial tilt angle for DIM (using an Olympus DIM microscope) was calculated after Yamamoto's formula [16] as follows; 39″ for a $\times 5$ objective lens, and 1′18″ for a $\times 10$ objective lens. The maximum interference contrast for DIM is achieved when the shearing direction of the polarizing prism is set perpendicular to the axis of the facial tilt. If the shearing direction of the prism in DIM is set parallel to the axis of the tilt, no contrast is created and one fails to detect a domain boundary, therefore it is not possible to see the whole field of veiw with the same sensitivity. In the case of PCM, however, one is able to observe the whole surface with an equal sensitivity with a

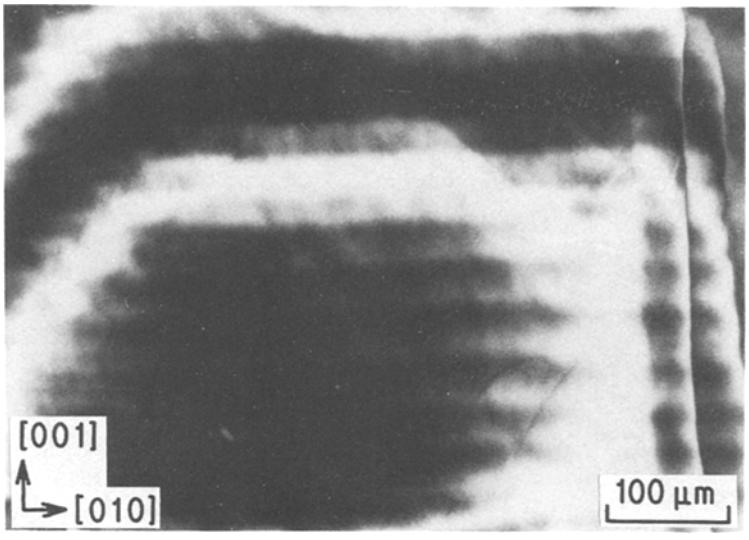

Figure 9 A high-dispersion interference contrast micrograph on a two-wall domain structure.

remarkable contrast, and the detection limit of the step height can go down to 1.5 nm [17].

The limit of the measurement of facial tilt angle using TBI depends on the height and width of the domain structure. For instance, if the width of a domain is 100 μm, the minimum angle that can be measured should be 7″.

In a twinned crystal where the distance between the T-walls is 100 μm or less the specular reflection technique begins to fail. However, the optical techniques applied in this work can go further and reveal the facial tilt angle on a small domain whose width is only 3 μm as shown in Fig. 7.

The highest lateral resolution of DIM and PCM is about 1 μm [11], whereas it is several microns for back-reflection X-ray topography [7] and more than 100 μm for neutron topography [15].

The optical methods introduced here exceed in resolution other techniques so far tried for visualizing the antiferromagnetic domains on a bulk crystal; in addition to this merit they are simple and non-destructive, and particularly suited to *in situ* observation of the behaviour of T-wall domains.

Acknowledgements

The authors would like to thank Emeritus Professor Takemaro Sakurai for his encouragement.

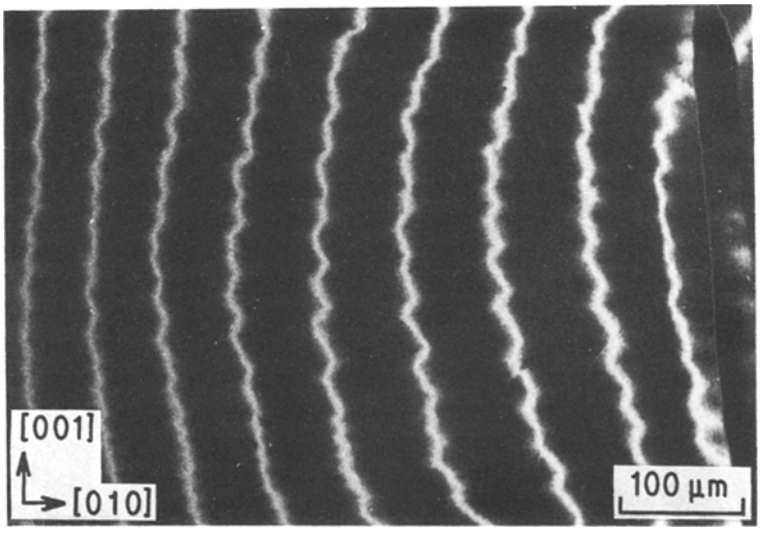

Figure 10 A two-beam interferogram on the same two-wall domain structure that was shown in Fig. 9, taken by a × 20 interference objective lens with monochromatic light of wavelength 546 nm.

References

1. M. FOEX, *Compt. Rend.* **227** (1948) 193.
2. C. H. LA BLANCHETAIS, *J. Phys. Radium* **12** (1951) 765.
3. H. P. ROOKSBY, *Acta Crystallogr.* **1** (1948) 226.
4. Y. SHIMOMURA and Z. NISHIYAMA, *Mem. Inst. Sci. and Industr. Res. Osaka Univ.* **6** (1948) 30.
5. G. A. SLACK. *J. Appl. Phys.* **31** (1960) 1571.
6. W. L. ROTH, *ibid.* **31** (1960) 2000.
7. S. SAITO, *J. Phys. Soc. Jpn* **17** (1962) 1287.
8. I. A. BLECH and E. S. MEIERAN, *Phil. Mag.* **14** (1966) 275.
9. K. KRANJC, *J. Appl. Crystallogr.* **2** (1969) 262.
10. M. ANDO, *Phys. Status Solidi (a)* **24** (1974) 473.
11. H. KOMATSU, Proceedings of the 2nd International Conference on Crystal Growth and Characterization, Japan, April 1974, edited by R. Ueda and J. B. Mullin (North-Holland, Amsterdam, 1975) p. 333.
12. T. SAKURAI and M. ISHIGAME, *J. Crystal Growth* **2** (1968) 284.
13. T. TAKEDA and H. KONDOH, *J. Phys. Soc. Jpn* **17** (1962) 1315.
14. S. TOLANSKY, "Surface Microtopography" (Longmans, London, 1960) p. 56.
15. J. BARUCHEL, M. SCHLENKER, K. KUROSAWA and S. SAITO, *Phil. Mag.* **B43** (1981) 853.
16. T. YAMAMOTO, *J. Jpn Soc. Precision Eng.* **31** (1965) 1008.
17. A. R. VERMA, *Phil. Mag.* **42** (1951) 1005.

Received 22 *November*
and accepted 19 *December* 1984